

Integrability and level crossing manifolds in a quantum Hamiltonian system

Vyacheslav V. Stepanov and Gerhard Müller

Department of Physics, University of Rhode Island, Kingston, Rhode Island 02881-0817

(Received 17 June 1998)

We consider a two-spin model, represented *classically* by a nonlinear autonomous Hamiltonian system with two degrees of freedom and a nontrivial integrability condition, and *quantum mechanically* by a real symmetric Hamiltonian matrix with invariant blocks of dimensionalities $K = \frac{1}{2}l(l+1)$, $l = 1, 2, \dots$. In the six-dimensional parameter space of this model, classical integrability is satisfied on a five-dimensional hypersurface, and level crossings occur on four-dimensional manifolds that are completely embedded in the integrability hypersurface except for some lower-dimensional submanifolds. Under mild assumptions, the classical integrability condition can be reconstructed from a purely quantum mechanical study of level degeneracies in finite-dimensional invariant blocks of the Hamiltonian matrix. Our conclusions are based on rigorous results for $K=3$ and on numerical results for $K=6, 10$. [S1063-651X(98)13711-X]

PACS number(s): 05.45.+b, 75.10.Hk, 75.10.Jm

I. INTRODUCTION

One of the most widely studied indicators of quantum chaos can be obtained via the statistical analysis of energy level spacings. Generically, the level spacings of quantized integrable systems tend to be well described by an exponential distribution (Poisson statistics), whereas quantized non-integrable systems tend to have a distribution in which the probability of very small spacings is suppressed (Wigner statistics) due to the phenomenon of level repulsion. The level turbulence such as exists in quantized nonintegrable systems can be simulated by the eigenvalues of random matrices with specific distributions of elements (e.g., Gaussian orthogonal ensemble) [1,2].

The statistical nature of this indicator precludes its use for mapping out the regions of integrability in the parameter space of Hamiltonian systems. However, determining the conditions for the occurrence of level degeneracies, on which the outcome of the statistical analysis depends, proves to be useful for precisely that purpose.

Here we show for a specific model system how the (known) classical integrability condition in a six-dimensional (6D) parameter space can be reconstructed, under mild assumptions, from a purely quantum mechanical study of the manifolds (in the same parameter space) where at least two energy levels are degenerate.

Practical considerations dictate that we use a model system where the Hilbert space splits into finite-dimensional invariant subspaces. However, the significance of the results presented here transcends this restriction and suggests that the concept of integrability remains meaningful albeit more subtle for quantum systems with few degrees of freedom [3,4].

We consider two quantum spins $\mathbf{S}_1, \mathbf{S}_2$ in biaxial orientational potentials interacting via a biaxial exchange coupling. The Hamiltonian reads

$$H = \sum_{\alpha=xyz} \left\{ -J_{\alpha} S_1^{\alpha} S_2^{\alpha} + \frac{1}{2} A_{\alpha} [(S_1^{\alpha})^2 + (S_2^{\alpha})^2] \right\}. \quad (1)$$

The spin operators $\mathbf{S}_l = (S_l^x, S_l^y, S_l^z)$ satisfy the commutation

relations $[S_l^{\alpha}, S_{l'}^{\beta}] = i\hbar \delta_{ll'} \sum_{\gamma} \epsilon_{\alpha\beta\gamma} S_l^{\gamma}$. Their time evolution is governed by the Heisenberg equation

$$\frac{d\mathbf{S}_l}{dt} = \frac{i}{\hbar} [H, \mathbf{S}_l], \quad l=1,2. \quad (2)$$

If both spins have the same quantum mechanical length $\sqrt{\sigma(\sigma+1)}$ ($\sigma = \frac{1}{2}, 1, \frac{3}{2}, \dots$), the discrete symmetry group of the Hamiltonian (1) is $D_2 \otimes S_2$, where D_2 contains all the twofold rotations C_2^{α} , $\alpha = x, y, z$ about the coordinate axes, and $S = (E, P)$ is the permutation group of the two spins. The characters of this group are displayed in Table I [5].

The use of symmetry-adapted basis vectors with transformation properties corresponding to the eight different irreducible representations R of $D_2 \otimes S_2$ brings the Hamiltonian matrix into block-diagonal form:

$$H = \bigoplus_{R, \sigma} H_R^{\sigma}. \quad (3)$$

There exist invariant subspaces with dimensionalities $K = 1, 3, 6, 10, \dots$ in 16 different realizations for four different values of the spin quantum number σ as illustrated in Table II. The case $K=1$ is exceptional.

TABLE I. The characters of the irreducible representations R of the group $D_2 \otimes S_2$.

$D_2 \otimes S_2$	E	C_2^z	C_2^y	C_2^x	P	PC_2^z	PC_2^y	PC_2^x
A1S	1	1	1	1	1	1	1	1
A1A	1	1	1	1	-1	-1	-1	-1
B1S	1	1	-1	-1	1	1	-1	-1
B1A	1	1	-1	-1	-1	-1	1	1
B2S	1	-1	1	-1	1	-1	1	-1
B2A	1	-1	1	-1	-1	1	-1	1
B3S	1	-1	-1	1	1	-1	-1	1
B3A	1	-1	-1	1	-1	1	1	-1

TABLE II. Dimensionalities K of the invariant subspaces pertaining to the eight symmetry classes R of eigenstates for spin quantum numbers $\sigma \leq 4$.

$R \setminus \sigma$	$\frac{1}{2}$	1	$\frac{3}{2}$	2	$\frac{5}{2}$	3	$\frac{7}{2}$	4
A1S		3	1	6	3	10	6	15
A1A	1		3	1	6	3	10	6
B1S	1	1	3	3	6	6	10	10
B1A		1	1	3	3	6	6	10
B2S	1	1	3	3	6	6	10	10
B2A		1	1	3	3	6	6	10
B3S	1	1	3	3	6	6	10	10
B3A		1	1	3	3	6	6	10

II. CLASSICAL INTEGRABILITY MANIFOLD

In the limit $\hbar \rightarrow 0$, $\sigma \rightarrow \infty$, $\hbar \sqrt{\sigma(\sigma+1)} = s$, the operators S_l^α become the components of the classical spin vector with fixed length s [6],

$$\mathbf{S}_l = (S_l^x, S_l^y, S_l^z) = s(\sin \vartheta_l \cos \varphi_l, \sin \vartheta_l \sin \varphi_l, \cos \vartheta_l), \quad (4)$$

and Eq. (2) turns into Hamilton's equation,

$$\frac{d\mathbf{S}_l}{dt} = -\mathbf{S}_l \times \frac{\partial H}{\partial \mathbf{S}_l} = \{H, \mathbf{S}_l\}, \quad l=1,2 \quad (5)$$

where $\{S_l^\alpha, S_{l'}^\beta\} = -\delta_{ll'} \sum_\gamma \epsilon_{\alpha\beta\gamma} S_l^\gamma$ are the Poisson brackets for spin variables. Each classical spin (4) is expressible in terms of two canonical coordinates

$$p_l = s \cos \vartheta_l, \quad q_l = \varphi_l, \quad l=1,2. \quad (6)$$

The Hamiltonian (1), now interpreted as a classical energy function, thus specifies an autonomous system with two degrees of freedom. Integrability of that system requires the existence of a second integral of the motion, i.e., an analytic function I of the spin components S_l^α with the property $\{I, H\} = 0$.

A systematic search for a second invariant in the form of a degree-two polynomial yielded two distinct nontrivial solutions, provided the six parameters satisfy the condition [7]

$$(A_x - A_y)(A_y - A_z)(A_z - A_x) + \sum_{\alpha\beta\gamma = \text{cycl}(xyz)} J_\alpha^2 (A_\beta - A_\gamma) = 0. \quad (7)$$

If there is no single-site anisotropy, $A_x = A_y = A_z$, then the second integral of motion reads

$$I = - \sum_{\alpha\beta\gamma = \text{cycl}(xyz)} J_\alpha J_\beta S_1^\gamma S_2^\gamma + \frac{1}{2} \sum_{\alpha = xyz} J_\alpha^2 [(S_1^\alpha)^2 + (S_2^\alpha)^2], \quad (8)$$

otherwise it has the form

$$I = \sum_{\alpha = xyz} g_\alpha S_1^\alpha S_2^\alpha,$$

$$g_\alpha = J_\alpha (J_\alpha + J_\beta + J_\gamma) + (A_\alpha - A_\beta) J_\gamma + (A_\alpha - A_\gamma) J_\beta - (A_\alpha - A_\beta)(A_\alpha - A_\gamma), \quad \alpha\beta\gamma = \text{cycl}(xyz). \quad (9)$$

Hence, in the 6D parameter space of this two-spin model the classical integrability condition is satisfied on a 5D manifold. Integrals of the motion of higher-degree polynomial form or of nonpolynomial form cannot be ruled out, but it is unlikely that any other hypersurface of integrability would have escaped the numerical studies of this model [7,8]. Additional integrability manifolds of dimensionalities four or less remain an intriguing possibility but do not interfere with any conclusions reached in this study.

III. LEVEL-CROSSING MANIFOLDS

Does the integrability condition (7) of the classical two-spin model (1) have any bearing on the presence or absence of level degeneracies in low-dimensional invariant subspaces of the corresponding quantum two-spin model? The subspaces with a single energy level ($K=1$), which are realized for $\sigma \leq 2$, are uninteresting in this context. The next lowest subspace dimensionality is $K=3$. The occurrence of level degeneracies for the parametric Hamiltonian (1) will now be analyzed on a rigorous basis for all 16 invariant subspaces with $K=3$. Their entries are highlighted in Table II.

A. Parametric representation for $K=3$

The most general real symmetric 3×3 matrix has six independent elements. For the purpose of studying level degeneracies, it is sufficient to consider matrices with zero trace:

$$M = \begin{pmatrix} 2h & b & d \\ b & e-h & c \\ d & c & -e-h \end{pmatrix}. \quad (10)$$

That leaves five independent elements b, c, d, e, h and thus simplifies the analysis because the characteristic polynomial now has a vanishing quadratic term:

$$|M - xE| = x^3 - Bx + C = 0. \quad (11)$$

The discriminant has the form

$$D = 4B^3 - 27C^2, \quad (12)$$

with coefficients

$$B = b^2 + c^2 + d^2 + e^2 + 3h^2, \quad (13)$$

$$C = h(2e^2 + 2c^2 - b^2 - d^2 - 2h^2) + e(d^2 - b^2) - 2bcd.$$

The zeros of D coincide with the points of level degeneracy in M . This is evident in the product form

$$D = \prod_{i < k} (x_i - x_k)^2 \quad (14)$$

of the discriminant in terms of the roots x_i of Eq. (11). Since D is non-negative and depends smoothly on b, c, d, e, h , its partial derivatives must also vanish at all points of level degeneracy:

$$\frac{\partial D}{\partial b} = 12B^2 2b - 54C(-2bh - 2eb - 2cd) = 0,$$

$$\frac{\partial D}{\partial c} = 12B^2 2c - 54C(4hc - 2bd) = 0,$$

$$\frac{\partial D}{\partial d} = 12B^2 2d - 54C(-2dh + 2ed - 2cb) = 0, \quad (15)$$

$$\frac{\partial D}{\partial e} = 12B^2 2e - 54C(4eh + d^2 - b^2) = 0,$$

$$\frac{\partial D}{\partial h} = 12B^2 6h - 54C(2e^2 + 2c^2 - b^2 - d^2 - 6h^2) = 0.$$

These additional conditions simplify the search for zeros of D . $C=0$ implies $B=0$ and vice versa. This case describes the threefold level degeneracy at $b=c=d=e=h=0$. Henceforth we assume $B \neq 0$ and $C \neq 0$ with no loss of generality. The five relations (15) can then be written in the more compact form

$$\begin{aligned} \frac{2B^2}{9C} &= \frac{-bh - be - cd}{b} = \frac{2hc - bd}{c} = \frac{-dh + ed - bc}{d} \\ &= \frac{4eh + d^2 - b^2}{2e} = \frac{2e^2 + 2c^2 - b^2 - d^2 - 6h^2}{6h}. \end{aligned} \quad (16)$$

Inspection shows that only two of the relations (16) are independent, and that $D=0$ holds wherever Eq. (16) is satisfied. The points of level crossing are thus confined to a 3D manifold in (b, c, d, e, h) space. This manifold can be parametrized by three of the five elements. For $e \neq 0$ and $b \neq \pm d$ we have

$$c = \frac{2bde}{b^2 - d^2}, \quad h = \frac{b^2 - d^2}{6e} \left[1 - \frac{2e^2(b^2 + d^2)}{(b^2 - d^2)^2} \right]. \quad (17)$$

Viewed on any of the five 4D coordinate hyperplanes, where one of the elements b, c, d, e, h is equal to zero, the level-crossing manifold reduces to two or three 2D surfaces. Parametric representations of all eight such surfaces are given in Table III.

B. Level crossing labels

In a three-level system, any twofold degeneracy either involves the upper two levels or the lower two levels. How does this distinction manifest itself in the structure of the level crossing manifold? The eigenvalues of the matrix M for points on the level crossing manifold can be written in the form

$$(x_1, x_2, x_3) = \left(\xi, -\frac{1}{2}\xi, -\frac{1}{2}\xi \right), \quad (18)$$

TABLE III. 2D intersections of the 3D level-crossing manifold (17) with the 4D coordinate hyperplanes. The two elements of Eq. (10) which play the role of parameters in each case are marked by asterisks.

b	c	d	e	h
0	0	*	*	$\frac{2e^2 - d^2}{6e}$
0	*	0	*	$\pm \frac{1}{3}\sqrt{e^2 + c^2}$
*	0	0	*	$\frac{b^2 - 2e^2}{6e}$
*	*	$\pm b$	0	$\pm \frac{b^2 - c^2}{3c}$
*	$\pm \frac{\sqrt{2}bd}{\sqrt{b^2 + d^2}}$	*	$\pm \frac{1}{\sqrt{2}} \frac{b^2 - d^2}{\sqrt{b^2 + d^2}}$	0

where

$$\xi = \frac{4}{3} \left[\frac{e(b^2 + d^2)}{b^2 - d^2} + \frac{b^2 - d^2}{4e} \right]. \quad (19)$$

If $\xi > 0$ ($\xi < 0$) then it is the highest (lowest) level that remains nondegenerate. A threefold degeneracy ($\xi = 0$) occurs only at the point $b = c = d = e = h = 0$.

Do the points with $\xi > 0$ and the points with $\xi < 0$ form connected regions on the level crossing manifold? To investigate this issue we consider the map described by Eq. (17) between the (b, d, e) space and the 3D level crossing manifold in (b, c, d, e, h) space. This map is singular on the three planes $e=0$, $b+d=0$, $b-d=0$, which divide the (b, d, e) space into octants. Octants which share a face (one quadrant of a coordinate plane) have ξ values of opposite sign, and octants which share only an edge (half a coordinate axis) have ξ values of equal sign.

For a point (b, d, e) approaching any one of the three planes that separate octants, the image in (b, c, d, e, h) space diverges, but for a point (b, d, e) approaching a line where any two of the three separating planes intersect, the image may or may not diverge.

Consider smooth trajectories of points (b, d, e) that connect two octants across one of these special lines. Inspection shows that any trajectory connecting octants with a common face has a divergent image. However, there do exist trajectories with nondivergent and continuous images between any two octants that have only an edge in common.

For example, set $b+d > 0$ and consider trajectories $e \rightarrow 0$, $b-d \rightarrow 0$ with $e/(b-d) = u \neq 0$ toward the edge of four octants. Along such a trajectory we have

$$c = bu, \quad h = \frac{b}{3u} - \frac{bu}{3}, \quad \xi = \frac{4bu}{3} + \frac{2b}{3u}. \quad (20)$$

Octants that are diagonally across the edge have either both $u > 0$ or $u < 0$. Hence they are connected by trajectories with finite c, h and with no change of sign in ξ . No such trajectories exist between adjacent octants.

TABLE IV. Dependence of $\lambda_R^\sigma = \text{Tr } H_R^\sigma$ and of the five independent matrix elements of $M = H_R^\sigma - \lambda_R^\sigma$ on the six parameters of Eq. (1) for four invariant blocks of Eq. (3) with $K=3$.

H_{A1S}^1	$\lambda = 2(A_x + A_y + A_z)/3$ $b = -(J_x + J_y)/\sqrt{2}$ $c = (A_x - A_y)/2$ $d = (J_y - J_x)/\sqrt{2}$ $e = -J_z$ $h = (A_x + A_y)/6 - A_z/3$
H_{A1A}^3	$\lambda = 4(A_x + A_y + A_z)$ $b = -3(J_x + J_y)/\sqrt{2}$ $c = 3(A_x - A_y)/2$ $d = 3(J_y - J_x)/\sqrt{2}$ $e = 3J_z$ $h = (A_x + A_y)/2 - A_z$
H_{B1S}^2	$\lambda = 11(A_x + A_y)/6 + 7A_z/3 - 5J_z/3$ $b = -\sqrt{3}(J_x + J_y)$ $c = \sqrt{3}(A_x - A_y)/2$ $d = J_y - J_x$ $e = (A_x + A_y)/2 - A_z + 2J_z$ $h = (A_x + A_y)/3 - 2A_z/3 + J_z/3$
H_{B1A}^2	$\lambda = 11(A_x + A_y)/6 + 7A_z/3 + 5J_z/3$ $b = \sqrt{3}(J_y - J_x)$ $c = \sqrt{3}(A_x - A_y)/2$ $d = -J_x - J_y$ $e = (A_x + A_y)/2 - A_z - 2J_z$ $h = (A_x + A_y)/3 - 2A_z/3 - J_z/3$

All this demonstrates that the 3D level crossing manifold consists of one sheet for $\xi < 0$ and one sheet for $\xi > 0$, connected only at the point $b = c = d = e = h = 0$.

C. Embedment in classical integrability manifold

These results can now be used to locate all level crossings in the invariant blocks of Eq. (3) with $K=3$. Table II identifies 16 such blocks, two for each symmetry class. The three eigenvalues of H_R^σ on the level crossing manifold are then

$$(E_1, E_2, E_3) = \left(\xi, -\frac{1}{2}\xi, -\frac{1}{2}\xi \right) + \lambda_R^\sigma, \quad (21)$$

with ξ given in Eq. (19). Table IV expresses $\lambda_R^\sigma = \text{Tr } H_R^\sigma$ and the matrix elements a, b, c, d, e, h in terms of the six Hamiltonian parameters for four of the 16 invariant subspaces of Eq. (3) with $K=3$.

Consider, for example, the matrix H_{A1A}^3 pertaining to the symmetry class A1A for spin quantum number $\sigma=3$. If we take one of the relations (16) which must be satisfied at all points of level crossing,

$$c(2e^2 + 2c^2 - b^2 - d^2 - 6h^2) = 6h(2ch - bd), \quad (22)$$

and express the matrix elements in terms of the Hamiltonian parameters for H_{A1A}^3 , we find that it is equivalent to the classical integrability condition (7). Hence no level crossings occur in H_{A1A}^3 if the classical system is nonintegrable. In the 6D parameter space of Eq. (1), the points of level degeneracy pertaining to H_{A1A}^3 are thus confined to a 4D manifold which is determined, according to Eq. (17), by the two relations

$$A_x - A_y = \frac{(J_x^2 - J_y^2)J_z^2}{J_x J_y J_z}, \quad (23)$$

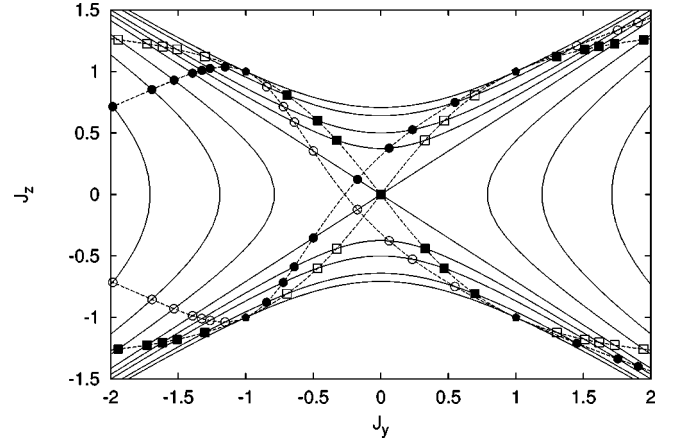


FIG. 1. The dashed curves are level crossing lines in the reduced parameter space (J_y, J_z, A) projected onto the (J_y, J_z) plane for two invariant blocks H_R^σ with $K=3$: H_{A1A}^3 (circles) and H_{B1S}^2 (squares). The solid lines represent the integrability hyperboloid at $|A| = 0, 0.3, 0.5, 0.6, 0.7, 1/\sqrt{2}, 0.9, 1.1, 1.4$. The pentagons mark symmetry points of H .

$$A_x + A_y - 2A_z = \frac{2J_x^2 J_y^2 - (J_x^2 + J_y^2)J_z^2}{J_x J_y J_z}.$$

Either relation can be replaced by the classical integrability condition (7).

We have determined that in all 16 invariant subspaces with $K=3$ the conditions (17) for the occurrence of a level degeneracy imply that the classical integrability condition (7) is satisfied. Geometrically speaking, the classical integrability condition is satisfied on a 5D hypersurface in 6D parameter space. In each of the 16 invariant $K=3$ subspaces of H , level crossings occur on a distinct 4D manifold. The result of our calculation is that all 16 4D *level-crossing manifolds* are embedded in the 5D *classical integrability hypersurface* of the 6D parameter space.

D. Shape for $K=3$

For a graphical representation of the level crossing manifolds embedded in the integrability manifold we use the reduced 3D parameter space spanned by $J_y, J_z, A_x - A_y \equiv 2A$ at $J_x = 1, A_x + A_y = 0, A_z = 0$ [9]. Here the integrability condition (7) reads

$$A(1 + J_y^2 - 2J_z^2 - 2A^2) = 0 \quad (24)$$

and is satisfied on two intersecting 2D surfaces—the plane $A=0$ and a hyperboloid. In any plane $A \neq 0$, integrability thus holds on a pair of hyperbolic curves. Several such lines are shown in Fig. 1. The two intersecting straight lines pertain to $A = \pm 1/\sqrt{2}$.

The level-crossing manifolds are lines in (J_y, J_z, A) space, embedded in the 2D integrability manifold (24). Table V gives parametric representations of the level-crossing lines in (J_y, J_z, A) space for four of the 16 H_R^σ blocks with $K=3$.

The dashed curves in Fig. 1 represent projections onto the (J_y, J_z) plane of the pairs of level-crossing lines pertaining to the invariant blocks H_{A1A}^3 and H_{B1S}^2 of Eq. (3). In

TABLE V. Level crossing lines with $\xi > 0$ (upper sign) and $\xi < 0$ (lower sign) in the reduced parameter space (J_y, J_z, A) of four invariant blocks of Eq. (3) with $K=3$.

H_{A1S}^1	$J_z = \frac{\pm\sqrt{2}J_y}{\sqrt{1+J_y^2}}$	$A = \frac{\pm(1-J_y^2)}{\sqrt{2(1+J_y^2)}}$
H_{A1A}^3	$J_z = \frac{\mp\sqrt{2}J_y}{\sqrt{1+J_y^2}}$	$A = \frac{\pm(1-J_y^2)}{\sqrt{2(1+J_y^2)}}$
H_{B1S}^2	$J_z = \frac{\pm(1+4J_y+J_y^2)}{\sqrt{10+16J_y+10J_y^2}}$	$A = \frac{\pm 2(1-J_y^2)}{\sqrt{10+16J_y+10J_y^2}}$
H_{B1A}^2	$J_z = \frac{\mp(1-4J_y+J_y^2)}{\sqrt{10-16J_y+10J_y^2}}$	$A = \frac{\pm 2(1-J_y^2)}{\sqrt{10-16J_y+10J_y^2}}$

(J_y, J_z, A) space, the two lines of each pair wrap around the integrability hyperboloid in such a way that one is the reflection image of the other with respect to the J_y axis. Points of intersection of the level crossing lines with planes $A = \text{const}$ are marked as full (open) symbols for $A > 0$ ($A < 0$).

We have investigated the level crossing manifolds for all 16 invariant blocks of H_R^σ with $K=3$ in the reduced parameter space. There exists exactly one level crossing line with $\xi > 0$ and one with $\xi < 0$ in each case. All lines are infinite and different from each other. Each line crosses the plane $A=0$ at two of the four symmetry points $(J_y, J_z) = (\pm 1, \pm 1), (\pm 1, \mp 1)$. These are the only points with $A=0$ where degenerate levels exist. Each level crossing line thus represents the 1D slice in (J_y, J_z, A) space of the sheet with $\xi > 0$ or $\xi < 0$ of one of the 16 4D level crossing manifolds for $K=3$.

E. Dimensionality for arbitrary K

Higher-dimensional Hamiltonian matrices exist in the two-spin model (1) as invariant blocks of Eq. (3) for $K = 6, 10, 15, \dots$ in 16 different realizations each. A real symmetric $K \times K$ matrix B has $\frac{1}{2}K(K+1)$ independent elements. On the level crossing manifold L of dimensionality d_L (to be determined), two or more of the K eigenvalues are degenerate. The manifold L maps onto a manifold Z of dimensionality $d_Z = d_L - 1$, where at least two eigenvalues are zero.

Two vanishing eigenvalues imply that all minors $|m_{ij}|$ of the determinant $|B|$ are zero, which yields K^2 relations among the matrix elements B_{ij} that must be satisfied. Not all relations are independent. The requirement $|m_{ij}| = |m_{ji}|$ renders $\frac{1}{2}K(K-1)$ relations redundant. For $K > 2$ another K relations are redundant because of the condition $\sum_i B_{ij} (-1)^{i+j} |m_{ij}| = |B| = 0$ [10]. That leaves $\frac{1}{2}K(K-1)$ independent relations for a guaranteed pair of zero-energy levels. Consequently, we have $d_Z = K$, i.e., $d_L = K + 1$. For $K = 3$ we thus recover the results of the explicit calculation, namely, a 4D level crossing manifold in a 6D space of independent matrix elements. Both dimensionalities are reduced by one if we impose the condition of zero trace.

In an alternative approach, the matrix B has two vanishing eigenvalues if the two lowest-order coefficients, C_0 and

C_1 , in the characteristic polynomial

$$|B - \lambda E| = \sum_{k=1}^K C_k \lambda^k \quad (25)$$

vanish [11]. They are sums of products of up to K and $K-1$ matrix elements, respectively. This condition is equivalent to the $\frac{1}{2}K(K-1)$ conditions that all minors $|m_{ij}|$ vanish. The equivalence of the two alternative criteria alerts us to the fact that the conditions $C_0 = C_1 = 0$ are compound conditions, each one equivalent to multiple conditions of the kind $|m_{ij}| = 0$ [12].

In the context of the two-spin model, all matrix elements are functions of six Hamiltonian parameters. Not all $\frac{1}{2}K(K-1) - 1$ relations which determine the level-crossing manifold are independent any more. All evidence suggests that there remain exactly two independent relations, which then describe a 4D manifold on the 5D integrability surface in 6D parameter space, no matter what the matrix dimensionality K is.

It is expected that the level crossing manifold of a system with K levels ($E_1 \leq E_2 \leq \dots \leq E_K$) consists of $K-1$ distinct 4D sheets where levels k and $k+1$ are degenerate. In the case $K=3$ we have indeed identified two sheets and labeled them by the sign of the energy parameter ξ .

The two independent relations among the Hamiltonian parameters which determine the 4D level crossing manifolds involve polynomials of degrees $\propto K$. The shape of the level crossing manifolds thus becomes increasingly convoluted as K grows larger. Any randomly picked path on the integrability manifold will thus intersect a given 4D sheet of a level-crossing manifold more and more frequently. As a consequence, the number of level crossing lines in the reduced parameter space will increase more rapidly than the numbers of levels present.

F. Shape for $K=6, 10$

Figure 2 depicts the level crossing manifold for the invariant block H_{A1A}^4 of Eq. (3) with $K=6$ levels in the reduced parameter space (J_y, J_z, A) . The representation is similar to that used in Fig. 1 for $K=3$. The data shown here are mainly the results of a numerical search for level crossings, but some of the level degeneracies thus identified can be corroborated analytically. The configuration of level crossing lines is reflection symmetric with respect to the lines $J_y = A = 0$ and $J_z = A = 0$.

Among the six levels with energies $E_1 \leq E_2 \leq \dots \leq E_6$, any occurrence of a level crossing can be characterized by the position $[k, k+1]$ of the two degenerate levels in the level sequence [13]. This label thus distinguishes five different kinds of level crossings. All level crossing lines shown in Fig. 2 are labeled accordingly. In the integrability plane $A=0$, level crossings occur at the four symmetry points $(J_y, J_z) = (\pm 1, \pm 1), (\pm 1, \mp 1)$ as was already the case for $K=3$, and along the two (dot-dashed) lines $J_y = 0$ and $J_z = 0$.

On the integrability hyperboloid we have identified ten level crossing lines (dashed curves) as compared to just two lines for $K=3$. All ten lines are infinite. Eight of them intersect the integrability plane at the four symmetry points men-

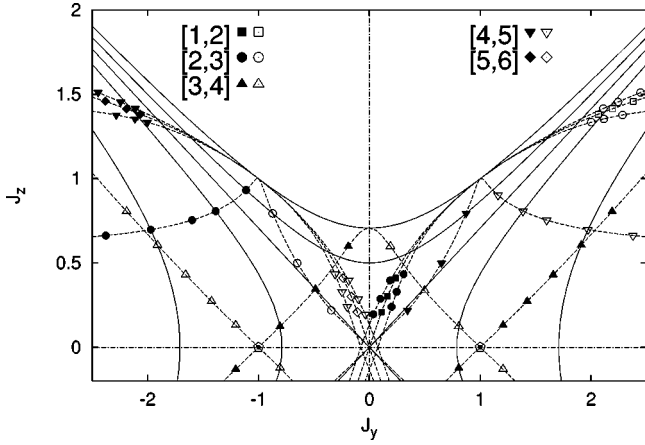


FIG. 2. The dashed curves are level crossing lines in (J_y, J_z, A) space projected onto the (J_y, J_z) plane for the invariant block H_{A1A}^4 with $K=6$: The solid lines represent the integrability hyperboloid at $A=0, 0.5, 1/\sqrt{2}, 0.9, 1.4$. The full (open) symbols mark degeneracies between levels k and $k+1$ (see legend) at $A>0$ ($A<0$). Level-crossing lines [3,4] in the integrability plane $A=0$ are shown dot-dashed. The pentagons mark the positions of two anomalous lines of [3,4] degeneracy perpendicular to the (J_y, J_z) plane.

tioned previously, where multiple degeneracies occur and are well understood [14]. The intersection points ($J_y=0, J_z = \pm 1/\sqrt{2}$) for the remaining two lines do not involve multiple level degeneracies.

Thus far the structure of the observed level-crossing manifold is in full accord with the scenario outlined in Sec. III E. However, there also exist two straight lines of level degeneracy oriented perpendicular to the (J_y, J_z) plane at $(J_y = \pm 1, J_z = 0)$. These two level crossing lines are not confined to the integrability manifold. They involve a degeneracy [3,4] at energy $E=0$ [5,15]. Most important in the context of our study is the dimensionality of this anomalous level crossing submanifold. Unlike the other level crossing lines in the reduced parameter space, which are slices of 4D structures in the full 6D parameter space, they remain lower dimensional.

The data for the invariant block H_{A1A}^5 of Eq. (3), which has $K=10$ levels, confirm all the essential features that we have already identified for the cases $K=3, 6$. New features that would necessitate any change in interpretation have not been observed. Figure 3 shows that the number of level crossing lines has increased to ten on the integrability plane $A=0$ (dot-dashed lines) and to 30 on the integrability hyperboloid (solid lines at $A>0$, dashed lines at $A<0$). As predicted, this increase exceeds the increase in the number of levels significantly.

Every level crossing line on the hyperboloid intersects the plane $A=0$ at least once, either at one of the symmetry points or at the intersection with a level crossing line in the plane. The two anomalous level crossing lines observed for $K=6$ at $(J_y = \pm 1, J_z = 0)$ are present again. All level crossing lines except the anomalous ones represent slices of what must be $K-1=9$ distinct sheets that make up the 4D level crossing manifold in 6D parameter space. This manifold remains fully embedded in the 5D classical integrability hypersurface (7). Only the anomalous submanifold sticks out into the classically nonintegrable region.

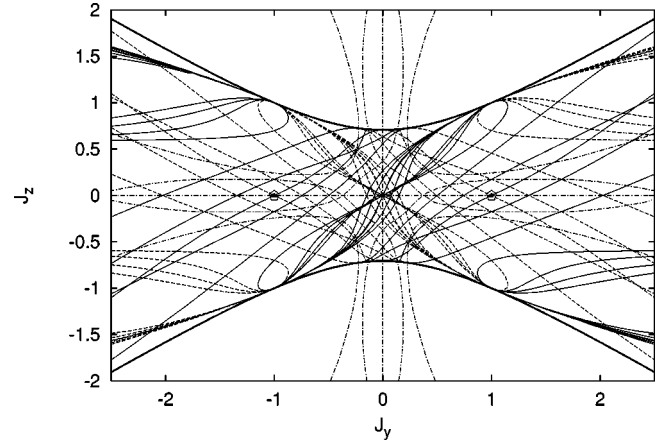


FIG. 3. Level crossing lines in (J_y, J_z, A) space for the invariant block H_{A1A}^5 with $K=10$. The solid (dashed) lines are projections onto the (J_y, J_z) plane of 30 level crossing lines at $A>0$ ($A<0$) on the integrability hyperboloid. The dot-dashed lines are ten level crossing lines in the integrability plane $A=0$. The thick lines outline the projected hyperboloid. The pentagons mark the positions of two anomalous lines of level degeneracy perpendicular to the (J_y, J_z) plane.

IV. QUANTUM INTEGRABILITY MANIFOLD

The picture that emerges from this study of level degeneracies in a quantum Hamiltonian system with a nontrivial classical integrability condition may be summarized as follows. (i) In the 6D parameter space of the two-spin model (1), level degeneracies occur predominantly on smooth 4D structures. (ii) For any given invariant block H_R^σ with K levels of the Hamiltonian matrix (3), this 4D structure consists of $K-1$ sheets, where each sheet represents one pair $[k, k+1]$ of degenerate levels in the sequence $E_1 \leq E_2 \leq \dots \leq E_K$. (iii) In addition to these 4D level crossing sheets there also exist lower-D structures in the 6D phase space on which level degeneracies take place. (iv) Level degeneracies involving more than two states, likewise, occur only on lower-D structures. For the most part they are observed at symmetry points of the Hamiltonian. (v) All $K-1$ 4D level crossing sheets pertaining to any invariant block H_R^σ are completely embedded in the 5D hypersurface on which the classical integrability condition (7) is satisfied. Only lower-D structures of the level crossing manifold exist elsewhere in parameter space.

These observations are remarkable in the context of the elusive concept of quantum integrability. One might argue that integrability in the sense of analytic solvability has no meaning for any matrix H_R^σ because algorithms that diagonalize real symmetric $K \times K$ matrices operate without any restrictions. The fact is, however, that a universal switch is encoded in all H_R^σ matrices that permits an abundance of level degeneracies on a smooth 5D hypersurface in 6D parameter space and prohibits them almost everywhere else, i.e., strictly everywhere else for $K=3$ and everywhere else except on lower-D submanifolds for $K>3$. As we carry out the analysis for more and more invariant blocks H_R^σ , the shape of this 5D hypersurface emerges with growing definition as the smooth interpolation of an ever increasing set of 4D level crossing sheets.

There is no *a priori* reason why the classical integrability condition (7) should have any such clear-cut bearing on the spectral properties of low-dimensional irreducible quantum representations of the two-spin model (1). On the basis of the correspondence principle, one might surmise that the 5D classical integrability hypersurface is only relevant quantum mechanically in an asymptotic sense, i.e., for systems with $\sigma \rightarrow \infty$. The fact is, however, that in some representations with as few as $K=3$ levels the classical integrability condition results naturally as one of two conditions that, in combination, guarantee a level degeneracy. Another fact is that (under mild assumptions) the classical integrability condition (7) can be reconstructed analytically from the quantum mechanical condition for the occurrence of level degeneracies within low- K invariant subspaces.

If the level crossing manifolds are described by polynomial equations among the Hamiltonian parameters as is the case here, then their compatibility with an integrability condition that is also described by a polynomial is restricted. Bézout's theorem [16] states (effectively) that the maximum number of independent 4D manifolds which are embedded simultaneously in two different 5D degree- n polynomial hypersurfaces in projective space is n^2 . Hence, the 16 independent 4D level-crossing manifolds in 6D parameter space that we have determined analytically for $K=3$ representations in Eq. (3) uniquely determine the 5D integrability manifold if it is described by a polynomial of degree less than $\sqrt{16}=4$. For the situation at hand, the classical integrability manifold is

thus the only degree-three polynomial that can accommodate all 16 level crossing manifolds for $K=3$. When we add the polynomial level crossing manifolds for $K=6,10,\dots$ to the set of embedded manifolds, the uniqueness of the integrability manifold applies to polynomials of higher and higher degree.

The relation (7) among the six Hamiltonian parameters is thus no less relevant for the quantum mechanical properties than it is for the classical mechanical properties of the two-spin model (1). It plays the role of a *quantum integrability manifold* as much as it represents the classical integrability manifold.

The fact that almost all level crossings are confined to this 5D hypersurface in 6D parameter space is a compelling indicator that *quantum integrability* is a meaningful concept for systems with few degrees of freedom. However, its essence has yet to be elucidated. A different indicator of quantum integrability and nonintegrability, which is based on tracking individual eigenvectors along closed paths through parameter space, is the subject of a study currently in progress and promises to shed further light on this issue [17].

ACKNOWLEDGMENTS

The work at URI was supported by NSF Grant No. DMR-93-12252. We are grateful to J. Stolze for useful comments on the manuscript.

-
- [1] M. C. Gutzwiller, *Chaos in Classical and Quantum Mechanics* (Springer-Verlag, New York, 1990).
- [2] L. E. Reichl, *The Transition to Chaos in Conservative Classical Systems: Quantum Manifestations* (Springer-Verlag, New York, 1992).
- [3] S. Weigert, *Physica D* **56**, 107 (1992).
- [4] S. Weigert and G. Müller, *Chaos Solitons Fractals* **5**, 1419 (1995).
- [5] R. Weber, Ph.D. thesis, University of Basel, 1988.
- [6] M. Månson, *Phys. Rev. B* **12**, 400 (1975); H.-D. Meyer and W. H. Miller, *J. Chem. Phys.* **71**, 2156 (1979).
- [7] E. Magyari, H. Thomas, R. Weber, C. Kaufman, and G. Müller, *Z. Phys. B* **65**, 363 (1987).
- [8] N. Srivastava, C. Kaufman, G. Müller, R. Weber, and H. Thomas, *Z. Phys. B* **70**, 251 (1988).
- [9] The J_α, A_α are measured in arbitrary energy units divided by \hbar^2 . Henceforth this unit will be suppressed in all explicit results.
- [10] No further redundancy is caused by the equivalent condition $\sum_j B_{ij}(-1)^{i+j}|m_{ij}|=|B|=0$.
- [11] The transformation $B_{ii} \rightarrow B_{ii} + \Delta E$, $i=1,\dots,K$ of the matrix elements on the diagonal makes any other energy hypersurface accessible to the same method of analysis.
- [12] The compound nature is already apparent for $K=2$: The two conditions $C_0=m_{11}m_{22}-m_{12}^2=0$, $C_1=-m_{11}-m_{22}=0$ are equivalent to the three conditions $m_{11}=m_{12}=m_{22}=0$.
- [13] The much scarcer events of multiple degeneracy will be discussed in passing, but they are of little importance in the context of this study.
- [14] N. Srivastava and G. Müller, *Z. Phys. B* **81**, 137 (1990).
- [15] Weber (Ref. [5]) showed that the energy level $E=0$ is $(2\sigma+1)$ -fold degenerate on the lines $(J_y=\pm 1, J_z=0)$ in the reduced parameter space, irrespective of whether the integrability condition is satisfied or not. For $\sigma \geq 2$, this number $(2\sigma+1 \geq 5)$ exceeds the number of symmetry classes $(A1A, A1S, B1S, B1A)$, where $E=0$ does occur. Hence, some eigenvectors within the same symmetry class must be degenerate. Weber also showed that for $A \neq 0$ the degeneracy of $E=0$ is completely removed away from the line $J_y=\pm 1$, no matter whether integrability is preserved or not.
- [16] P. Griffiths and J. Harris, *Principles of Algebraic Geometry* (Wiley, New York, 1978); K. Kendig, *Elementary Algebraic Geometry* (Springer-Verlag, New York, 1977); I. R. Shafarevich, *Foundations of Algebraic Geometry*, 2nd ed. (Nauka, Moscow, 1988), Vol. 1.
- [17] V. V. Stepanov and G. Müller (unpublished).